RESEARCH ARTICLE

MicroRNA-888-3p impairs sperm motility in patients with asthenozoospermia by inhibiting IGF2 receptor expression

Mengli Cui[1], Jianing Zhang[1], Jiaqi Chen[1], Tingting Yu[1], Jing Yu[1], Jiacheng Zhang[1], Jinfeng Li[2, *], Zhijian Zhu[1, *]

[1]College of Biological and Food Engineering, [2]Affiliated Central Hospital, Huanghuai University, Zhumadian, Henan 463000, China.

Received: July 26, 2026. **Accepted:** October 30, 2026. **Published:** November 2, 2026.

Asthenozoospermia is a leading cause of male infertility with its underlying molecular mechanisms remaining largely undefined. MicroRNAs (miRNAs) are key post-transcriptional regulators of sperm function. This study aimed to identify key miRNAs associated with sperm motility. Small RNA sequencing was performed on pooled spermatozoa from 21 patients with asthenozoospermia and 21 normozoospermic controls, revealing 13 differentially expressed miRNAs. Among these, hsa-miR-888-3p exhibited the most pronounced upregulation and the highest abundance in patient spermatozoa, a finding corroborated by quantitative real-time PCR (qRT-PCR). Integrative bioinformatic predictions combined with dual-luciferase reporter assays confirmed that hsa-miR-888-3p directly targeted the 3'-untranslated region (3'-UTR) of the insulin-like growth factor 2 receptor (IGF2R) and suppressed its expression. Functional studies in GC-1 spermatogonia cells demonstrated that IGF2R knockdown enhanced GSK3β phosphorylation, reduced ATP and total antioxidant status (TAS), and attenuated superoxide dismutase (SOD) and glutathione S-transferase (GST) activities, mirroring the metabolic and oxidative disturbances observed in patient spermatozoa. Notably, overexpression of hsa-miR-888-3p recapitulated these effects, indicating that hsa-miR-888-3p-mediated inhibition of IGF2R impaired sperm motility by dysregulating energy metabolism and antioxidant defense. Collectively, these findings established a novel hsa-miR-888-3p/IGF2R/GSK3β regulatory axis that governed sperm motility and highlighted hsa-miR-888-3p as a potential diagnostic biomarker and therapeutic target for asthenozoospermia.

Keywords: asthenozoospermia; miRNAs; insulin-like growth factor-II receptor; energy metabolism; antioxidant.

[*]**Corresponding authors:** Zhijian Zhu, College of Biological and Food Engineering, Huanghuai University, No.76 Kaiyuan Road, Yicheng District, Zhumadian, Henan 463000, China. Jinfeng Li, Affiliated Central Hospital, Huanghuai University, No.747 Zhonghua Road, Yicheng District, Zhumadian, Henan 463000, China. Email: luckzhuzhijian@163.com (Zhu Z). jinfengli202512@163.com. (Li J).

Introduction

In recent years, significant lifestyle changes, the progressive accumulation of environmental pollutants, and mounting psychosocial stress have driven a sustained decline in male semen quality, posing a significant challenge to public health and global population dynamics [1]. Asthenozoospermia, a predominant clinical phenotype of male infertility, accounts for over 30% of male infertility cases. Characterized by markedly impaired sperm motility, this condition not only reduces the success rate of natural fertilization but also contributes to embryo implantation failure and lower pregnancy rates in assisted reproductive technology (ART) [2].

Clinically, asthenozoospermia is divided into an isolated subtype, defined solely by motility impairment, and a syndromic subtype accompanied by multisystem abnormalities. The maintenance of sperm motility relies critically on the structural integrity of the flagellum [3], sufficient energy supply [4], and precise coordination among multiple signaling pathways [5]. A comprehensive understanding of its genetic basis and pathogenic mechanisms is essential for elucidating the etiology of this disorder.

The proper execution of sperm functions relies heavily on fine-tuned regulation at the post-transcriptional level. Previous studies have demonstrated that functional RNAs enriched in spermatozoa, particularly small non-coding RNAs, play essential roles in regulating sperm motility, capacitation, and early embryonic development [6]. As key mediators of post-transcriptional regulation, microRNAs (miRNAs) have been closely linked to various male infertility phenotypes through their dysregulated expression. With the widespread application of high-throughput sequencing technologies, numerous aberrantly expressed miRNAs have been identified in spermatozoa from patients with asthenozoospermia [7, 8], which are significantly associated with key signaling pathways including PI3K-Akt, MAPK, HIF-1, and FoxO, suggesting that they constitute a complex and crucial regulatory network governing sperm motility [9]. Previous studies reported that cysteine-rich secretory protein 2 (CRISP2), localized in the acrosome and flagellum of spermatozoa, participated in flagellar movement, acrosome reaction, and gamete fusion by regulating calcium influx. Aberrantly elevated miR-27a in spermatozoa suppressed CRISP2 expression, leading to abnormal sperm morphology and reduced motility [10]. In addition, miR-151a-5p interfered with sperm energy metabolism by reducing the levels of adenosine triphosphate (ATP) and cytochrome b (Cytb) [11], while miR-525-3p was involved in the pathogenesis of asthenozoospermia through regulation of semenogelin 1 (SEMG1) [12]. Our previous work also revealed that hsa-miR-7-5p, which was highly expressed in seminal plasma exosomes of asthenozoospermia patients, directly targeted RAF1 and modulated sperm motility through the RAF1-mediated MAPK signaling network [13]. Collectively, these lines of evidence indicate that miRNA regulatory axes represent a core component of the pathogenic mechanisms underlying asthenozoospermia, and that intervention targeting specific miRNAs has emerged as a highly promising research direction in this field.

To systematically investigate the molecular mechanisms underlying asthenozoospermia, this research conducted genome-wide miRNA expression profiling by using high-throughput sequencing on spermatozoa from asthenozoospermia patients and fertile controls. Subsequent bioinformatics predictions combined with experimental validation were performed to confirm the target and effect of miR-888-3p. The results of this study illustrated the role of the miR-888-3p/IGF2R regulatory axis in the pathogenesis of asthenozoospermia and elucidated the causal relationship and molecular mechanisms by which aberrant gene expression led to sperm dysfunction, thereby providing new theoretical insights and potential therapeutic targets for the diagnosis and treatment of this condition.

Materials and methods

Patient recruitment

Twenty-one (21) asthenozoospermic men aged 18 – 48 years were recruited with the criteria of sperm concentration > 15 × 10^6/mL, progressive motility (grade a + b) < 32%, and total motility < 40%. Additionally, 21 age-matched fertile men with normal semen parameters were included as controls. Participants with varicocele, urogenital infections, reproductive tract infections, or current or former smokers were excluded. All procedures of this research were approved by the Medical Ethics Committee of Zhumadian Central Hospital (Zhumadian, Henan, China).

Table 1. Sequences of primer pairs specific to qRT-PCR.

Name	Sequence (5′ – 3′)
hsa-miR-888-3p reverse-transcribed	CTCAACTGGTGTCGTGGAGTCGGCAATTCAGTTGAGTTCACCCA
hsa-miR-483-5p reverse-transcribed	CTCAACTGGTGTCGTGGAGTCGGCAATTCAGTTGAGCTCCCTTC
hsa-miR-185-3p reverse-transcribed	CTCAACTGGTGTCGTGGAGTCGGCAATTCAGTTGAGGACCAGAG
hsa-miR-136-3p reverse-transcribed	CTCAACTGGTGTCGTGGAGTCGGCAATTCAGTTGAGAGACTCAT
qRT-PCR-hsa-miR-888-3p-F	ACACTCCAGCTGGGGGACTGACACCTCTTTG
qRT-PCR-hsa-miR-483-5p-F	ACACTCCAGCTGGGGAAGACGGGAGGAAAGA
qRT-PCR-hsa-miR-185-3p-F	ACACTCCAGCTGGGGAGGGGCTGGCTTTCCT
qRT-PCR-hsa-miR-136-3p-F	ACACTCCAGCTGGGGCATCATCGTCTCAAAT
qRT-PCR-miR-universal-R	CTCAACTGGTGTCGTGGAGTCGGCAATTCAG
qRT-PCR-U6-F	CTCGCTTCGGCAGCACA
qRT-PCR-U6-R	AACGCTTCACGAATTTGCGT

Seminal collection and RNA isolation

Fresh semen samples were collected from each participant after a 2- to 3-day abstinence period. Total RNA was extracted from sperm pellets using TRIzol® Reagent (Life Technologies, Carlsbad, CA, USA) according to the manufacturer's protocol. RNA purity (A_{260}/A_{280} ratio) and concentration were measured using a NanoDrop ND-2000 spectrophotometer (Thermo Scientific, Waltham, MA, USA). RNA integrity was evaluated by determining the RNA integrity number (RIN) with an Agilent 2100 Bioanalyzer (Agilent Technologies, Santa Clara, CA, USA).

High-throughput sequencing

To obtain sufficient RNA for library construction, two pooled RNA samples were prepared from spermatozoa of asthenozoospermia patients and fertile controls. Total RNAs extracted from 21 patient samples and 21 control samples were pooled at equal concentrations and then subjected to Illumina sequencing in duplicate to identify differentially expressed miRNAs between the patient and control groups. Small RNA libraries were constructed using the TruSeq Small RNA Sample Preparation Kit v2 (Illumina, San Diego, CA, USA) according to the manufacturer's instructions to capture small RNAs bearing 3′-OH and 5′-P modifications. 1 µg of RNA was used for library preparation. The libraries were sequenced on an Illumina HiSeq 4000 platform. Data analysis was performed by using FastQC (http://www.bioinformatics.babraham.ac.uk/projects/fastqc/) and Trimmomatic (http://www.usadellab.org/cms/?page=trimmomatic) for quality control and filtering, miRDeep2 (https://www.mdc-berlin.de/content/mirdeep2) for read mapping and counting, and edgeR (https://bioconductor.org/packages/release/bioc/html/edgeR.html) and R (https://www.r-project.org/) software for differential expression analysis. Differentially expressed miRNAs were further filtered to identify potential biomarkers for asthenozoospermia using the criteria of $|\log_2$ fold change$| \geq 1$ with at least a 2-fold difference between patient and control groups and adjusted $P \leq 0.05$ (Benjamini–Hochberg correction).

RNA-Seq validation by quantitative real time polymerase chain reaction (qRT-PCR)

Based on the sequencing results, the four most upregulated miRNAs of hsa-miR-483-5p, hsa-miR-888-3p, hsa-miR-185-3p, and hsa-miR-136-3p were selected for further validation by qRT-PCR. The validation cohort comprised the same 21 patients with asthenozoospermia and 21 normozoospermic controls used in the sequencing phase. Stem-loop reverse transcription primers specific to each miRNA along with U6 primers were used for cDNA synthesis with the PrimeScript™ II First-Strand cDNA Synthesis Kit (TaKaRa, Kusatsu, Shiga, Japan). Real-time PCR was performed on an Applied Biosystems StepOnePlus™ Real-Time PCR System (Thermo Fisher Scientific, Waltham, MA, USA) using the SYBR® Premix Ex Taq™ II Kit (TaKaRa). The Bulge-Loop™ miRNA qRT-PCR

Primer Sets including one RT primer and a pair of qPCR primers for each miRNA and U6 primers were synthesized by Shanghai GenePharma Co., Ltd. (Shanghai, China) (Table 1). The PCR cycling conditions were 95°C for 30 s followed by 40 cycles of 95°C for 5 s and 60°C for 30 s. Melting curve analysis was performed using the default instrument settings. U6 small nuclear RNA was used as the endogenous reference for normalization. All reactions were performed in triplicate, and at least three independent experiments were conducted.

Target gene prediction

TargetScan (https://www.targetscan.org/vert_71/), miRmap (https://mirmap.ezlab.org/app), and miRDB (https://mirdb.org/) were used to comprehensively predict potential target genes of the differentially expressed miRNAs, and the results were integrated by using ANOROAD (https://mc.solargenomics.com/cloud-tool/drawing-tool/list). In addition, asthenozoospermia-related gene information was retrieved from the NCBI Gene database (https://www.ncbi.nlm.nih.gov/gene) to further prioritize candidate genes associated with male infertility.

Cell culture

HEK-293T cells and GC-1 spermatogonia cells (ATCC, Manassas, VA, USA) were cultured in DMEM/F12 medium supplemented with 10% fetal bovine serum (FBS) (Gibco, Thermo Fisher Scientific, Waltham, MA, USA), 100 U/mL penicillin, and 100 µg/mL streptomycin. Both cell lines were maintained at 37°C in a humidified atmosphere containing 5% CO_2. The medium was refreshed every 2 – 3 days, and cells were passaged upon reaching 80% – 90% confluence.

Dual-luciferase reporter assay

Target validation assays were performed in HEK-293T cells. The wild-type and mutant 3′-UTRs of the candidate target genes containing the miR-888-3p binding sites were cloned into the psiCHECK-2 vector (Promega, Madison, WI, USA) *via* Not I and Xho I sites to construct the dual-luciferase reporter plasmids. 200 ng of each wild-type or mutant 3′-UTR dual-luciferase reporter plasmids were co-transfected with 50 nM miRNA mimic or negative control (NC) mimic into HEK-293T cells seeded in 48-well plates using Lipofectamine™ 2000 reagent (Invitrogen, Thermo Fisher Scientific, Waltham, MA, USA). At 48 hours post-transfection, cells were washed twice with phosphate-buffered saline (PBS) (pH 7.4) and lysed with 20 µL of 1× passive lysis buffer (PLB) (Promega, Madison, WI, USA) for 15 minutes at room temperature. Firefly and Renilla luciferase activities were measured using the Dual-Luciferase® Reporter Assay System on a GloMax® 20/20 Luminometer (Promega, Madison, WI, USA). All experiments were performed in three independent biological replicates, each with three technical replicates. Data were presented as mean ± standard deviation (SD), and the relative luciferase activity for each construct was normalized to that of the NC group.

siRNA and miRNA transfection

The siRNA sequences used in this study were siR-IGF2R-1 (5′-AUC AUA AUA UGA AAG CUU CGC-3′), siR-IGF2R-2 (5′-ACA UAA GUC GCC AUC AAC GUA-3′), and siR-IGF2R-3 (5′-AUA UAU CGG GGU CAA AUA CCC-3′). The sequence of the hsa-miR-888-3p mimic was 5′-GAC UGA CAC CUC UUU GGG UGA A-3′. Cells were seeded in 6-well plates at a density of 2.5×10^4 cells/mL and cultured to 60% – 70% confluence prior to transfection. Transfection was performed using Lipofectamine™ RNAiMAX (Invitrogen, Thermo Fisher Scientific, Waltham, MA, USA) according to the manufacturer's instructions. Transfection efficiency was confirmed by qRT-PCR at 24 h and 48 h post-transfection. Cells were harvested at the indicated time points for subsequent RNA and protein extraction.

Quantitative real-time PCR analysis of IGF2R mRNA expression

Total RNAs were extracted from GC-1 cells, spermatozoa of normozoospermic controls, and spermatozoa of asthenozoospermia patients to quantify IGF2R mRNA expression levels by using TRIzol® Reagent (Life Technologies, Carlsbad, CA,

USA) followed by reverse transcription and qRT-PCR analysis. GAPDH was used as the endogenous reference gene for normalization. The primer sequences used for qRT-PCR were GAPDH forward (5′-AGG TCG GTG TGA ACG GAT TTG-3′), GAPDH reverse (5′-TGT AGA CCA TGT AGT TGA GGT CA-3′), IGF2R forward (5′-AGG TGA AGC CCA ACG ATC AG-3′), and IGF2R reverse (5′-CAT CGA GAT CGC CGT CTT GA-3′). Each reaction was performed in triplicate, and relative expression levels were calculated using the $2^{-\Delta\Delta Ct}$ method.

Western blot analysis

Sperm cell samples or GC-1 cells were lysed in RIPA buffer (Solarbio, Beijing, China) supplemented with protease inhibitors (Roche Diagnostics, Indianapolis, IN, USA) to prepare whole-cell extracts. Protein concentrations were determined by using a Micro BCA Protein Assay Kit (Thermo Fisher Scientific, Waltham, MA, USA). The lysates were mixed with SDS-PAGE loading buffer, separated by 10% SDS-PAGE, and transferred onto PVDF membranes. The membranes were blocked with 5% nonfat milk and incubated with protein-specific primary antibodies at 4°C overnight followed by incubation with HRP-conjugated secondary antibodies at room temperature for 2 h. Chemiluminescent signals were detected using a Western blotting chemiluminescence reagent (PerkinElmer, Shelton, CT, USA) and recorded with a Vilber Lourmat imaging system (Vilber Lourmat, Collégien, France). The protein-specific primary antibodies used in this experiment were anti-IGF2R rabbit monoclonal antibody (1:1,000) (Abcam, Cambridge, UK), anti-GSK3β rabbit monoclonal antibody (1:1,000) (Cell Signaling Technology, Danvers, MA, USA), anti-phospho-GSK3β (Ser9) rabbit monoclonal antibody (1:1,000) (Cell Signaling Technology, Danvers, MA, USA), and anti-ACTB mouse monoclonal antibody (1:1,000) (Sangon Biotech, Shanghai, China). At least three independent biological replicates were performed for each assay.

Measurement of ATP and total antioxidant status (TAS) content

Total cellular ATP content was measured using a luciferase-luciferin ATP Assay Kit (Beyotime Biotech Inc., Shanghai, China) according to the manufacturer's instructions. Briefly, cells were lysed with lysis buffer and centrifuged, and the supernatant was collected. 100 µL of ATP assay working solution was added to each well of a 96-well plate and incubated at room temperature for 5 min. After adding 20 µL of sample or ATP standard solution, luminescence intensity was measured using a GloMax™ 96 Microplate Luminometer (Promega). ATP levels were normalized to protein content and expressed as µmol/g protein. TAS, reflecting the total enzymatic and non-enzymatic antioxidant capacity, was evaluated using a commercial TAS kit (Randox Laboratories Ltd., Crumlin, County Antrim, UK) adapted to a Cobas Mira Autoanalyzer (Roche Diagnostics, Indianapolis, IN, USA). This method is based on the formation of the ABTS radical cation ($ABTS^{\bullet+}$) at 600 nm in the presence of peroxidase (metmyoglobin) and H_2O_2 [14, 15]. TAS values were expressed as µmol/mg protein.

Measurement of SOD and GST activity

Cells were homogenized in pre-cooled PBS using a glass homogenizer. SOD (Beyotime Biotech Inc., Shanghai, China) and GST (EBC-K278-S, Elabscience, Wuhan, China) activities were determined using the corresponding assay kits. Enzyme activities were normalized to total protein content and expressed as U/mg protein for SOD and U/mg protein or U/g protein for GST, as specified by the respective kit instructions. All measurements were performed in triplicate.

Statistical analysis

All statistical analyses were performed using SPSS software (IBM, Armonk, NY, USA). Unpaired two-tailed Student's t-tests were used to compare differences between experimental groups. *P* values less than 0.05 indicated statistically significant difference, while *P* values less than 0.01 indicated very significant difference. The *P* values were corrected using the Benjamini–Hochberg method to control the false discovery rate (FDR).

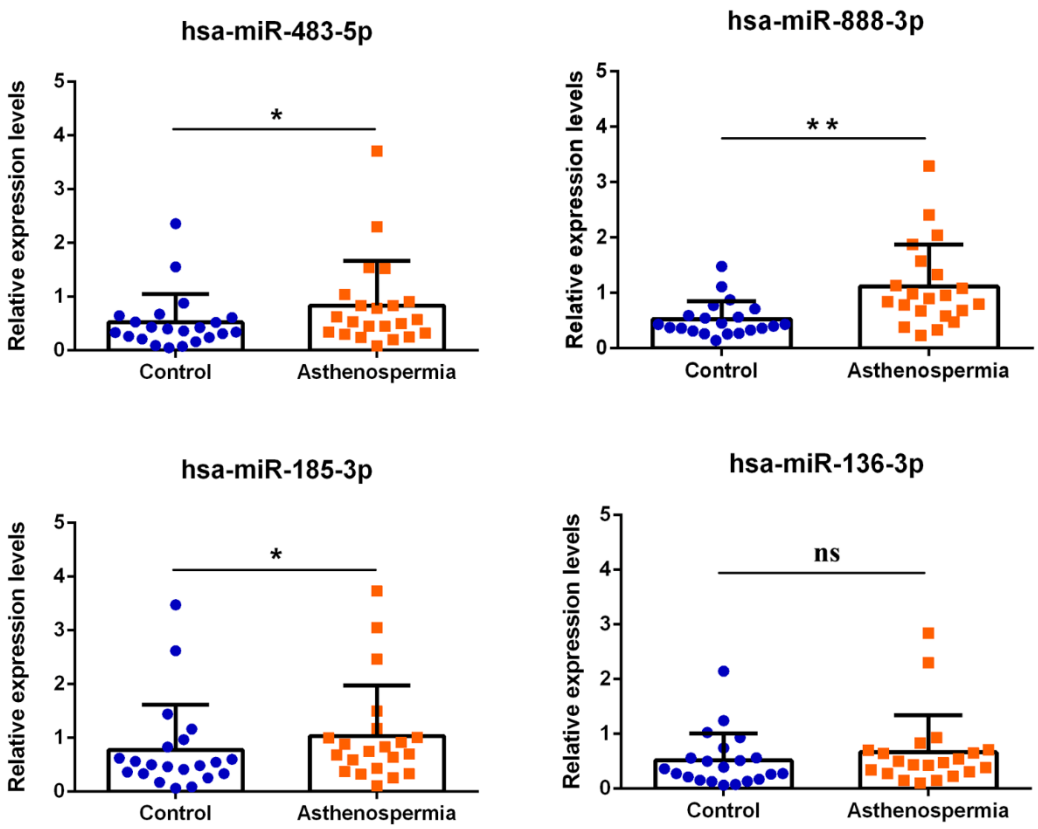


Figure 1. Relative expression levels of the four most significantly upregulated miRNAs (hsa-miR-483-5p, hsa-miR-888-3p, hsa-miR-185-3p, and hsa-miR-136-3p) in spermatozoa from normozoospermic controls (n = 21) and asthenozoospermia patients (n = 21). Data were presented as mean ± SD. $^{*}P < 0.05$, $^{**}P < 0.001$ *vs*. normozoospermic controls.

Results

Analysis of miRNA expression in normozoospermic and asthenozoospermic spermatozoa

Thirteen (13) miRNAs met the inclusion criteria of $|\log_2$ fold change$| \geq 1$ and adjusted $P \leq 0.05$. Among them, hsa-miR-483-5p, hsa-miR-888-3p, hsa-miR-185-3p, and hsa-miR-136-3p showed the most pronounced upregulation and were selected for further validation. The results demonstrated that hsa-miR-483-5p, hsa-miR-888-3p, and hsa-miR-185-3p were significantly upregulated in spermatozoa from asthenozoospermia patients compared with normozoospermic controls, whereas hsa-miR-136-3p exhibited an upward trend that did not reach statistical significance (Figure 1).

Prediction and screening of target genes of differentially expressed miRNAs

hsa-miR-888-3p exhibited the most pronounced differential expression and the highest abundance among all dysregulated miRNAs and, therefore, was prioritized for subsequent functional studies. Three online prediction tools including TargetScan, miRmap, and miRDB wereemployed to predict candidate target genes of hsa-miR-888-3p and yielded 3,350 (TargetScan), 986 (miRmap), and 500 (miRDB) candidate targets, respectively. Intersection analysis of the three datasets identified 204 common target genes (Figure 2). The top 15 genes with the highest prediction scores among the 204 common targets were selected for DLRA to evaluate the interaction between hsa-miR-888-3p and the predicted binding sites within the 3′-UTRs of these candidate genes. The DLRA results demonstrated that, compared with

the negative control (NC) mimic, hsa-miR-888-3p significantly suppressed the relative luciferase activity of reporter plasmids containing the 3′-UTRs of KLF3, ZFP36L1, RAP2A, S100PBP, FOXJ3, and IGF2R (Figure 3), suggesting that these six genes were potential direct targets of hsa-miR-888-3p.

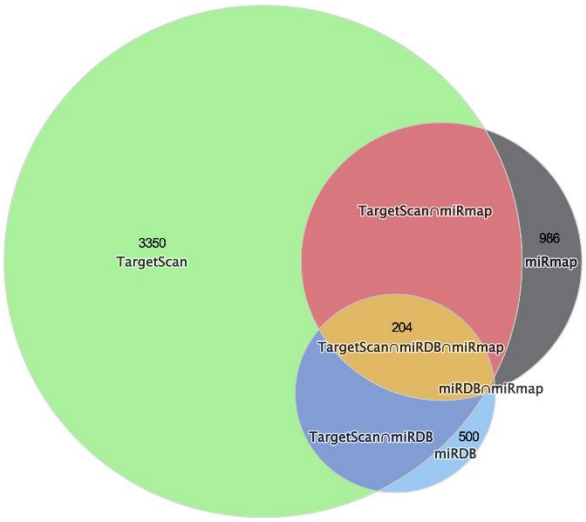


Figure 2. Venn diagram illustrating the overlap of predicted target genes of hsa-miR-888-3p among three independent bioinformatic tools. The intersection of the three datasets yielded 204 common candidate target genes.

Validation of hsa-miR-888-3p targeting of a sperm motility-related gene

The molecular functions of the six candidate target genes were analyzed. IGF2R, a key regulator of the IGF signaling pathway, was identified as a potential contributor to normal sperm function [16]. Site-directed mutagenesis dual-luciferase reporter assays were therefore performed to determine whether the regulatory effect of hsa-miR-888-3p on IGF2R was sequence-dependent. Mutation of the seed sequence-binding site in the IGF2R 3′-UTR abolished the inhibitory effect of hsa-miR-888-3p. Accordingly, the mutant reporter (mut-IGF2R-3′-UTR) no longer responded to hsa-miR-888-3p (Figure 4A). The IGF2R expression changes in GC-1 cells overexpressing hsa-miR-888-3p were further examined. qRT-PCR analysis revealed that overexpression of hsa-miR-888-3p significantly reduced IGF2R mRNA levels at 24 and 48 hours post-transfection, and Western blot analysis further confirmed marked downregulation of IGF2R protein expression (Figure 4B). To clarify the clinical relevance of this regulatory axis, IGF2R expression was compared between spermatozoa from normozoospermic controls (sperm motility ≥ 32%) and asthenozoospermia patients (sperm motility < 32%). Both qRT-PCR and Western blot analyses demonstrated that IGF2R mRNA and protein levels were significantly lower in the asthenozoospermia group than that in the normozoospermia group (Figure 4C). Collectively, these findings suggested that hsa-miR-888-3p might regulate sperm motility through targeted suppression of IGF2R expression.

Functional exploration of IGF2R in spermatozoa from asthenozoospermia patients

Upon binding to IGF2, IGF2R activates downstream signaling pathways involved in cellular glucose uptake and ATP production and plays a critical role in scavenging reactive oxygen species (ROS) and maintaining redox homeostasis [14]. Oxidative stress is well recognized to compromise sperm quality by inducing lipid peroxidation, DNA damage, and mitochondrial dysfunction, ultimately leading to reduced motility and fertilizing capacity [17, 18]. In this study, ATP content was significantly reduced in spermatozoa from asthenozoospermia patients compared to normozoospermic controls. Given that sperm flagellar motility is highly dependent on mitochondria-derived ATP, this result suggested that IGF2R might influence sperm motility through the regulation of energy metabolism. Furthermore, assessment of the ROS scavenging system revealed that total antioxidant status (TAS) was significantly lower in asthenozoospermia spermatozoa than in controls, accompanied by markedly decreased SOD and GST activities, indicating a disruption of redox balance (Figure 5). Previous studies have demonstrated that IGF2R modulates GSK3β activity by regulating its phosphorylation level,

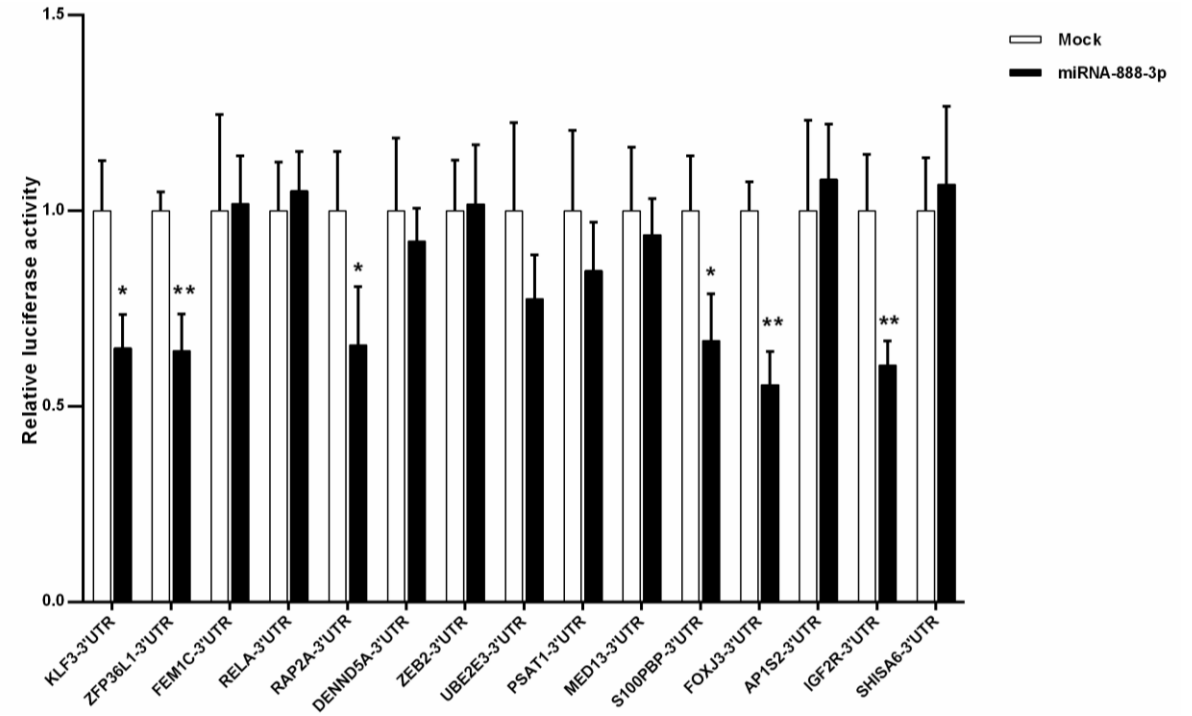


Figure 3. Dual-luciferase reporter assay (DLRA) evaluating the interaction between hsa-miR-888-3p and the 3′-UTRs of the top 15 candidate target genes. Data were presented as mean ± SD. $^{*}P < 0.05$, $^{**}P < 0.001$ *vs*. NC mimic.

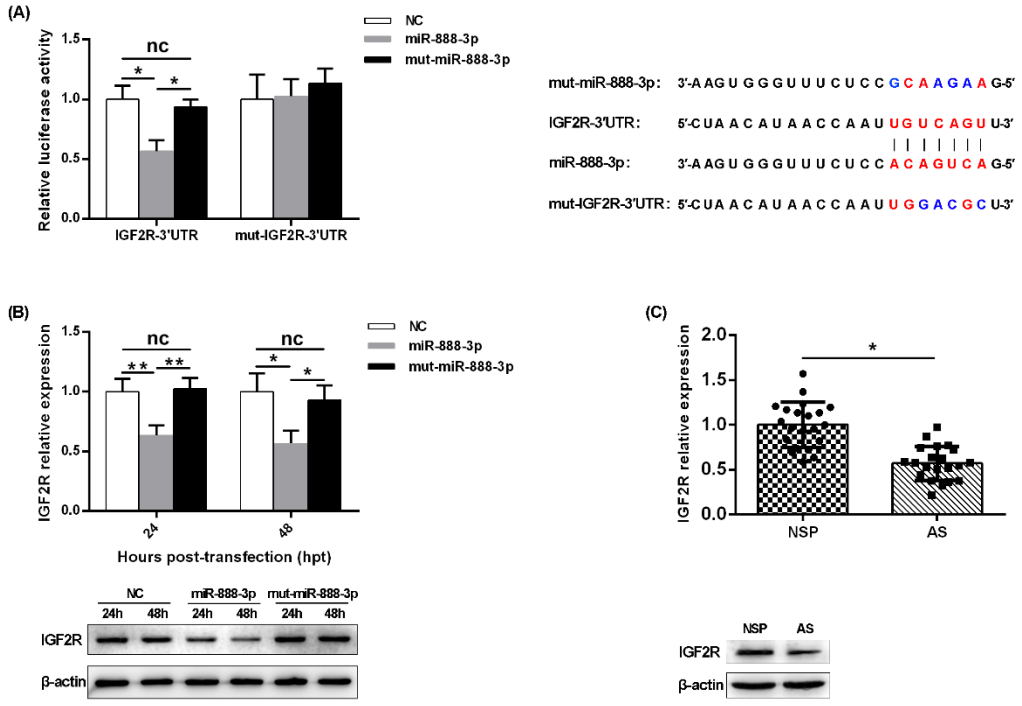


Figure 4. Validation of IGF2R as a direct target of hsa-miR-888-3p. **(A)** Dual-luciferase reporter assay confirming the interaction between hsa-miR-888-3p and the IGF2R 3′-UTR. The predicted seed sequence binding site within the IGF2R 3′-UTR (WT) and the corresponding mutant sequence (MUT) were shown on the right. **(B)** IGF2R mRNA and protein expression levels in GC-1 cells overexpressing hsa-miR-888-3p. **(C)** IGF2R mRNA and protein expression levels in spermatozoa from normozoospermic controls (NSP) and asthenozoospermia patients (AZS). Data were presented as mean ± SD. $^{*}P < 0.05$, $^{**}P < 0.001$ *vs*. normozoospermic controls.

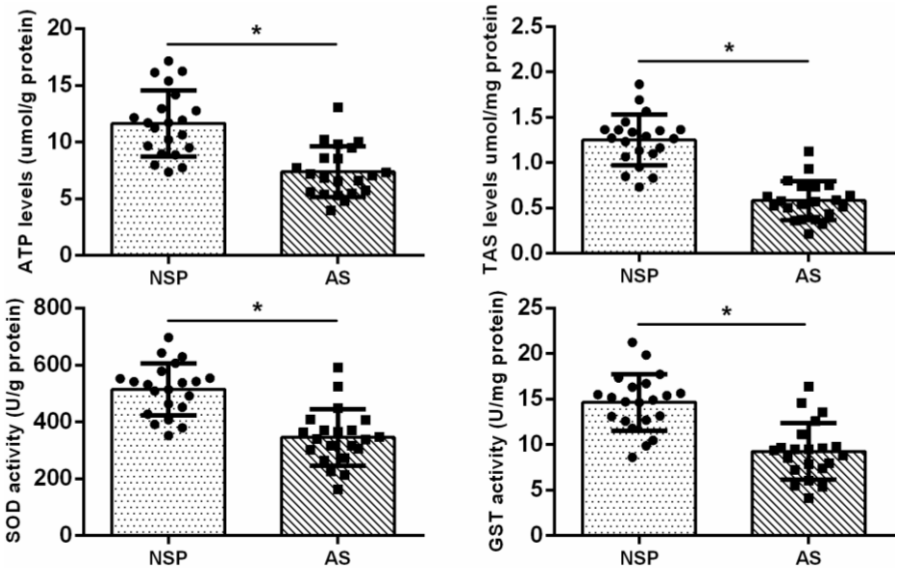


Figure 5. Evaluation of energy metabolism and antioxidant status in spermatozoa from asthenozoospermia patients. Data were presented as mean ± SEM (n = 3 independent experiments). $^{*}P < 0.05$, $^{**}P < 0.001$ *vs*. normozoospermic controls.

thereby participating in energy metabolism and antioxidant stress responses [19, 20]. To further validate the role of this regulatory axis in sperm function, IGF2R was knocked down in GC-1 cells, and the phosphorylation level of GSK3β, a key downstream effector of the IGF2/IGF2R signaling axis, was examined. The results showed that IGF2R knockdown significantly enhanced GSK3β (Ser9) phosphorylation (Figure 6A). Concurrently, ATP and TAS levels were markedly reduced, and SOD and GST activities were also suppressed (Figure 6B, 6C). These cellular findings were consistent with the observations in clinical samples, further supporting the notion that IGF2R participates in energy metabolism and antioxidant stress responses through regulation of GSK3β activity.

Functional study of hsa-miR-888-3p targeting IGF2R

Overexpression of hsa-miR-888-3p significantly reduced ATP and TAS levels and suppressed SOD and GST activities in GC-1 cells (Figure 7A). The IGF2R protein expression and GSK3β phosphorylation levels in GC-1 cells overexpressing hsa-miR-888-3p demonstrated that, compared with the mutant mimic or NC mimic, hsa-miR-888-3p suppressed IGF2R protein expression and significantly increased the level of phosphorylated GSK3β (Ser9) (Figure 7B), indicating inhibition of GSK3β activity. Collectively, these findings suggested that hsa-miR-888-3p regulated sperm motility in asthenozoospermia patients by targeting and suppressing IGF2R expression, thereby modulating energy metabolism and antioxidant stress responses in spermatozoa.

Discussion

In the present study, the miRNA expression landscape in spermatozoa from asthenozoospermia patients was systematically profiled by using Illumina high-throughput sequencing with the aim of identifying critical miRNA regulators implicated in sperm motility. Differential expression analysis revealed 13 miRNAs that met the stringent filtering criteria, among which the four most markedly upregulated candidates were further validated by qRT-PCR. Notably, hsa-miR-888-3p not only exhibited the most pronounced and consistent overexpression in patient spermatozoa but also displayed the highest abundance among all dysregulated miRNAs, underscoring its potential

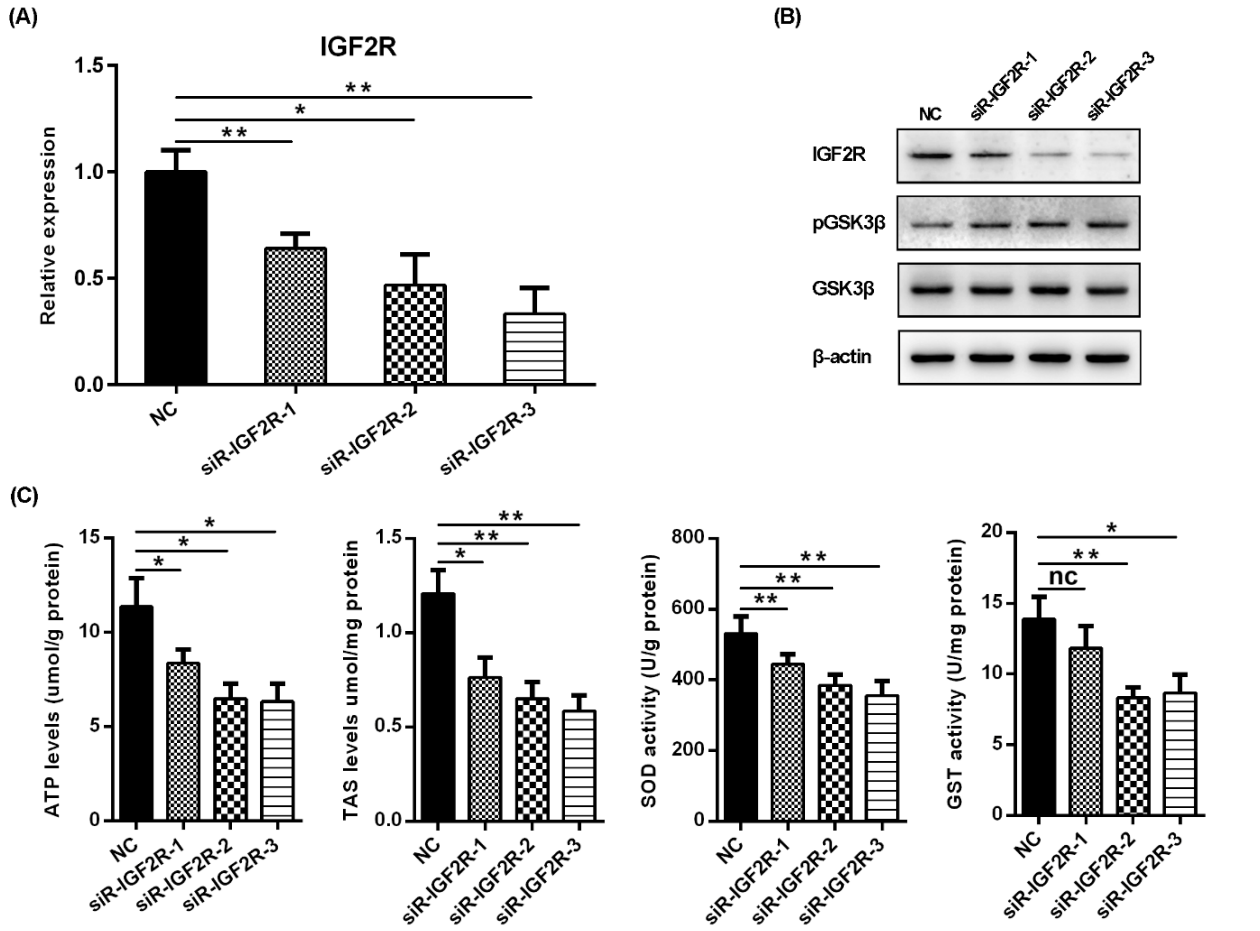


Figure 6. Effects of IGF2R knockdown on energy metabolism and antioxidant status in GC-1 cells. **(A)** IGF2R mRNA expression levels in GC-1 cells. **(B)** Western blot analysis of IGF2R protein expression and GSK3β phosphorylation (Ser9) levels in GC-1 cells. **(C)** ATP, TAS levels and SOD, GST activities in GC-1 cells. Data were presented as mean ± SD (n = 3 independent experiments). $^{*}P < 0.05$, $^{**}P < 0.001$ *vs*. NC.

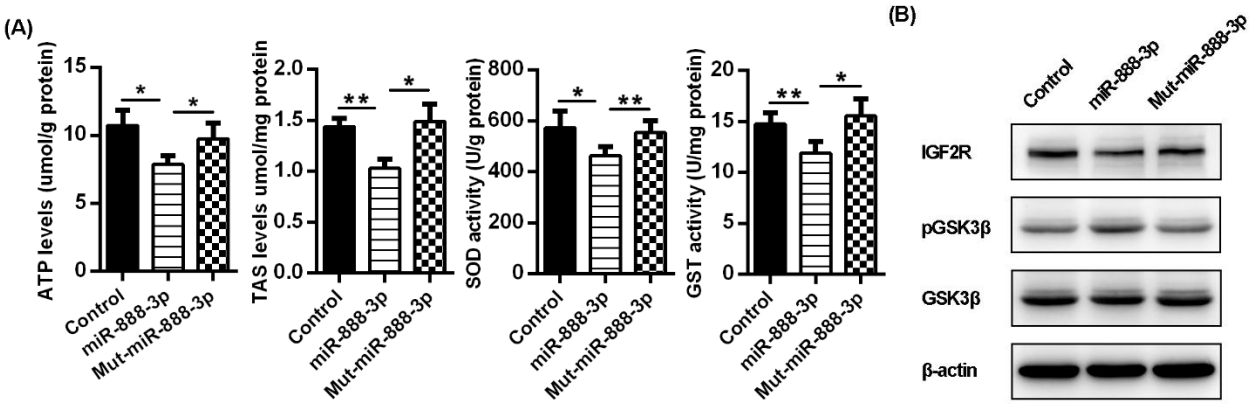


Figure 7. Effects of hsa-miR-888-3p overexpression on energy metabolism and antioxidant status in GC-1 cells. **(A)** ATP, TAS levels and SOD, GST activities in GC-1 cells. **(B)** Western blot analysis of IGF2R protein expression and GSK3β phosphorylation (Ser9) levels in GC-1 cells. Data were presented as mean ± SD (n = 3 independent experiments). $^{*}P < 0.05$, $^{**}P < 0.001$ *vs*. control.

biological relevance in the pathophysiology of asthenozoospermia. Given that spermatozoa enter a transcriptionally quiescent state after leaving the testis, their functional competence, particularly motility acquisition and fertilizing ability, is largely governed by post-transcriptional regulatory mechanisms including miRNA mediated modulation [21], as well as by epididymal microenvironmental cues delivered *via* exosomal RNA transfer [22]. In this context, hsa-miR-888-3p, which belongs to the epididymis enriched miR-888 cluster, was thought to be predominantly derived from epididymal epithelial cells, raising the possibility that it might exert regulatory functions during the terminal phases of sperm maturation. Previous high-throughput miRNA profiling studies have reported altered expression of hsa-miR-888-3p in spermatozoa from patients with asthenozoospermia [23]. This miRNA is encoded within the X-linked miR-888 cluster, a locus that is highly conserved among humans and non-human primates [24]. The cluster comprises seven miRNA genes and is predominantly enriched in epididymal epithelial cells, suggesting a potential role in post-testicular sperm maturation [25]. In a cohort of 69 patients with idiopathic asthenozoospermia, Qing *et al*. identified aberrant expression of five epididymis-specific miRNAs including miR-888 and further demonstrated that their expression levels significantly correlated with progressive sperm motility [26]. The results of this study were consistent with those of Heidary *et al*. who also revealed a marked upregulation of hsa-miR-888-3p in spermatozoa from asthenozoospermic individuals [23]. Conversely, several other studies have reported decreased levels of hsa-miR-888-5p in semen or seminal plasma samples [27]. These conflicting observations likely stem from a combination of technical and biological factors including differences in detection platforms, heterogeneity in specimen types, limited RNA input, insufficient biological replicates, and the intrinsic molecular heterogeneity of idiopathic asthenozoospermia. Collectively, these discrepancies underscore the urgent need to validate miRNA signatures in well-characterized samples under rigorously standardized experimental conditions.

To dissect the downstream molecular circuitry through which hsa-miR-888-3p exerted its regulatory influence on sperm motility, three independent bioinformatic tools including TargetScan, miRmap, and miRDB were employed to predict its potential target genes. Intersection analysis of the predictions yielded 204 common target genes, which were subsequently subjected to dual-luciferase reporter screening. This approach successfully identified six genes as direct targets of hsa-miR-888-3p including KLF3, ZFP36L1, RAP2A, S100PBP, FOXJ3, and IGF2R. Among these, IGF2R, a central modulator of the insulin-like growth factor (IGF) signaling axis, emerged as a particularly compelling candidate, given its established roles in cellular metabolism and redox regulation. Upon ligand binding, IGF2R initiates signaling cascades that facilitate proton translocation from the plasma membrane to mitochondria, thereby steering cellular metabolism toward oxidative phosphorylation and augmenting ATP production [20]. Additionally, the IGF2/IGF2R axis has been shown to enhance mitochondrial functional integrity as reflected by increased activities of manganese superoxide dismutase and cytochrome c oxidase along with elevated mitochondrial membrane potential [14]. Beyond its metabolic functions, this signaling axis also contributes to the scavenging of reactive oxygen species and the preservation of intracellular redox homeostasis [28]. Importantly, following IGF2 engagement, IGF2R modulates the phosphorylation status of GSK3β, a multifunctional kinase that serves as a key node integrating energy metabolism and antioxidant defense pathways [29]. To experimentally validate the functional relevance of this axis in sperm physiology, IGF2R expression in GC-1 spermatogonia cells was knocked down, which resulted in markedly enhanced GSK3β phosphorylation (indicative of its inactivation), accompanied by significant reductions in intracellular ATP levels, total antioxidant capacity, and the activities of superoxide dismutase and glutathione S-transferase. These

phenotypes closely recapitulated the metabolic and oxidative perturbations observed in spermatozoa from asthenozoospermia patients. Notably, ectopic overexpression of hsa-miR-888-3p produced a strikingly similar pattern as the suppression of IGF2R protein expression and concurrent elevation of GSK3β phosphorylation, mimicking the effects of direct IGF2R silencing. Collectively, these lines of evidence converged to define a functionally coherent "hsa-miR-888-3p–IGF2R–GSK3β" regulatory axis, wherein hsa-miR-888-3p mediated suppression of IGF2R relieved its inhibitory constraint on GSK3β phosphorylation, thereby perturbing the delicate balance between energy production and oxidative defense in sperm cells. Notably, the functions of IGF2R extended well beyond the regulation of energy metabolism and oxidative stress. Endoplasmic reticulum (ER) stress is a critical pathological process that can trigger apoptosis in male germ cells [30]. As a lysosomal targeting receptor, IGF2R possesses a unique ability to alleviate ER stress by mediating the trafficking and lysosomal degradation of its ligands, thereby facilitating the clearance of misfolded proteins and consequently inhibiting ER stress-induced germ cell apoptosis [31]. Therefore, a key question warranting further investigation is whether aberrant overexpression of hsa-miR-888-3p through suppression of IGF2R also plays a significant role in regulating sperm cell apoptosis, which represents an important direction for future studies.

This study has several limitations. The qRT-PCR validation of differentially expressed miRNAs was performed on the same cohort used for the RNA-seq discovery phase. While this approach provided robust technical confirmation of the sequencing data, it did not constitute an independent cohort validation of the biomarkers' clinical utility. Therefore, the conclusion that hsa-miR-888-3p served as a potential biomarker for asthenozoospermia remained exploratory and awaited confirmation in large-scale, independent, multicenter prospective cohort studies. Further, the functional mechanistic experiments in this study were primarily conducted in cell models. The complete regulatory network of the hsa-miR-888-3p/IGF2R axis within the *in vivo* spermatogenic microenvironment requires further validation using animal models. Furthermore, spermatozoa as highly differentiated and transcriptionally quiescent cells may differ significantly from somatic cells in terms of exogenous miRNA uptake efficiency and the functional regulatory mode of endogenous miRNAs, which warrants special attention in future investigations. This study systematically characterized the differentially expressed miRNA profile in spermatozoa from asthenozoospermia patients through high-throughput sequencing combined with molecular biological validation and delineated the functional role of the hsa-miR-888-3p/IGF2R/GSK3β signaling axis in the regulation of sperm motility. hsa-miR-888-3p was significantly overexpressed in spermatozoa of asthenozoospermia patients and directly suppressed IGF2R protein translation by targeting its 3'-UTR, thereby relieving the regulatory effect of IGF2R on GSK3β activity and ultimately leading to impaired energy metabolism and disruption of the antioxidant system in spermatozoa. This finding not only provided a new theoretical explanation for the molecular etiology of idiopathic asthenozoospermia but also identified IGF2R as a critical node linking metabolic reprogramming and redox homeostasis in spermatozoa. From a translational perspective, hsa-miR-888-3p as the most significantly differentially expressed miRNA in asthenozoospermic spermatozoa holds dual potential as both a diagnostic biomarker and a therapeutic target.

Acknowledgements

This work was supported by the Scientific and Technological Research Project Foundation of Henan Provincial Scientific and Technological Department (Grant No. 262102310075).

References

1. Akhatova A, Jones C, Coward K, Yeste M. 2025. How do lifestyle and environmental factors influence the sperm epigenome? Effects on sperm fertilizing ability, embryo development, and offspring health. Clin Epigenetics. 17(1):7.
2. Cavarocchi E, Drouault M, Ribeiro JC, Simon V, Whitfield M, Touré A. 2025. Human asthenozoospermia: Update on genetic causes, patient management, and clinical strategies. Andrology. 13(5):1044-1064.
3. Cavarocchi E, Whitfield M, Saez F, Touré A. 2022. Sperm ion transporters and channels in human asthenozoospermia: Genetic etiology, lessons from animal models, and clinical perspectives. Int J Mol Sci. 23(7):3926.
4. Shi S, Tang X, Long S, Yang J, Wang T, Wang H, *et al*. 2025. A novel homozygous LRRC6 mutation causes male infertility with asthenozoospermia and primary ciliary dyskinesia in humans. Andrology. 13(3):459-472.
5. Hu J, Li G, Ouyang B, Wang A, Li Y, Lu H. 2026. Morinda officinalis oligosaccharides improves sperm motility *via* the gut microbiota and the IGF-1/PI3K/mTOR signaling pathway. Front Endocrinol (Lausanne). 16:1711475.
6. Joshi M, Sethi S, Mehta P, Kumari A, Rajender S. 2023. Small RNAs, spermatogenesis, and male infertility: A decade of retrospect. Reprod Biol Endocrinol. 21(1):106.
7. Joshi M, Andrabi SW, Yadav RK, Sankhwar SN, Gupta G, Rajender S. 2022. Qualitative and quantitative assessment of sperm miRNAs identifies hsa-miR-9-3p, hsa-miR-30b-5p and hsa-miR-122-5p as potential biomarkers of male infertility and sperm quality. Reprod Biol Endocrinol. 20(1):122.
8. Burgos CF, Cikutovic R, Alarcón M. 2022. MicroRNA expression in male infertility. Reprod Fertil Dev. 34(12):805-818.
9. Liang G, Wang Q, Zhang G, Li Z, Wang Q. 2022. Differentially expressed miRNAs and potential therapeutic targets for asthenospermia. Andrologia. 54(1):e14265.
10. Zhou JH, Zhou QZ, Yang JK, Lyu XM, Bian J, Guo WB, *et al*. 2017. MicroRNA-27a-mediated repression of cysteine-rich secretory protein 2 translation in asthenoteratozoospermic patients. Asian J Androl. 19(5):591-595.
11. Zhou R, Wang R, Qin Y, Ji J, Xu M, Wu W, *et al*. 2015. Mitochondria-related miR-151a-5p reduces cellular ATP production by targeting CYTB in asthenozoospermia. Sci Rep. 5:17743.
12. Zhou QZ, Guo XB, Zhang WS, Zhou JH, Yang C, Bian J, *et al*. 2019. Expressions of miR-525-3p and its target gene SEMG1 in the spermatozoa of patients with asthenozoospermia. Andrology. 7(2):220-227.
13. Zhu ZJ, Cui ML, Yuan WJ, Zhang JN, Zhang S, Yao XQ, *et al*. 2025. Seminal plasma exosomal miRNA profiling reveals hsa-miR-7-5p as a key regulator of sperm motility in asthenozoospermia. Andrology. 14(7):2166-2179.
14. Martin-Montañez E, Pavia J, Santin LJ, Boraldi F, Estivill-Torrus G, Aguirre JA, *et al*. 2014. Involvement of IGF-II receptors in the antioxidant and neuroprotective effects of IGF-II on adult cortical neuronal cultures. Biochim Biophys Acta Mol Basis Dis. 1842(7):1041-1051.
15. Pasquali-Ronchetti I, Garcia-Fernandez MI, Boraldi F, Quaglino D, Gheduzzi D, De Vincenzi Paolinelli C, *et al*. 2006. Oxidative stress in fibroblasts from patients with pseudoxanthoma elasticum: Possible role in the pathogenesis of clinical manifestations. J Pathol. 208(1):54-61.
16. Tang P, Wang J, Tang X, Li Y, Li S. 2025. Insulin-like growth factor 2 in spermatogenesis dysfunction (Review). Mol Med Rep. 31(5):129.
17. Kaltsas A. 2023. Oxidative stress and male infertility: The protective role of antioxidants. Medicina (Kaunas). 59(10):1769.
18. Shayestehyekta M, Mohammadi T, Soltani L, Pooyanmehr M. 2026. Vitamin D3 protects ram epididymal sperm from oxidative stress and improves 4°C storage quality. Andrologia. 8230638.
19. Chen DY, Stern SA, Garcia-Osta A, Saunier-Rebori B, Pollonini G, Bambah-Mukku D, *et al*. 2011. A critical role for IGF-II in memory consolidation and enhancement. Nature. 469(7331):491-497.
20. Wang X, Lin L, Lan B, Wang Y, Du L, Chen X, *et al*. 2020. IGF2R-initiated proton rechanneling dictates an anti-inflammatory property in macrophages. Sci Adv. 6(48):eabb7389.
21. de Mateo S, Sassone-Corsi P. 2014. Regulation of spermatogenesis by small non-coding RNAs: Role of the germ granule. Semin Cell Dev Biol. 29:84-92.
22. Murdica V, Giacomini E, Alteri A, Bartolacci A, Cermisoni GC, Zarovni N, *et al*. 2019. Seminal plasma of men with severe asthenozoospermia contain exosomes that affect spermatozoa motility and capacitation. Fertil Steril. 111(5):897-908. e2.
23. Heidary Z, Zaki-Dizaji M, Saliminejad K, Khorram Khorshid HR. 2019. MicroRNA profiling in spermatozoa of men with unexplained asthenozoospermia. Andrologia. 51(6):e13284.
24. Belleannée C. 2015. Extracellular microRNAs from the epididymis as potential mediators of cell-to-cell communication. Asian J Androl. 17(5):730-736.
25. Hu L, Wu C, Guo C, Li H, Xiong C. 2014. Identification of microRNAs predominately derived from testis and epididymis in human seminal plasma. Clin Biochem. 47(10-11):967-972.
26. Qing X, Shi J, Dong T, Wu C, Hu L, Li H. 2017. Dysregulation of an X-linked primate-specific epididymal microRNA cluster in unexplained asthenozoospermia. Oncotarget. 8(34):56839-56849.
27. Barceló M, Mata A, Bassas L, Larriba S. 2018. Exosomal microRNAs in seminal plasma are markers of the origin of azoospermia and can predict the presence of sperm in testicular tissue. Hum Reprod. 33(6):1087-1098.
28. Martín-Montañez E, Millon C, Boraldi F, Garcia-Guirado F, Pedraza C, Lara E, *et al*. 2017. IGF-II promotes neuroprotection and neuroplasticity recovery in a long-lasting model of oxidative damage induced by glucocorticoids. Redox Biol. 13:69-81.
29. Chen Y, Xu D, Ma Y, Chen P, Hu J, Chen D, *et al*. 2023. Sertoli cell-derived extracellular vesicles traverse the blood-testis barrier and deliver miR-24-3p inhibitor into germ cells improving sperm mobility. J Control Release. 362:58-69.
30. Huang KH, Weng TI, Huang HY, Huang KD, Lin WC, Chen SC, *et al*. 2012. Honokiol attenuates torsion/detorsion-induced

testicular injury in rat testis by way of suppressing endoplasmic reticulum stress-related apoptosis. Urology. 79(4):967. e5-11.

31. Zhang B, Brahma RK, Zhu L, Feng J, Hu S, Qian L, *et al*. 2023. Insulin-like growth factor 2 (IGF2)-fused lysosomal targeting chimeras for degradation of extracellular and membrane proteins. J Am Chem Soc. 145(44):24272-24283.